ELSEVIER

Measurement of fission product yields in the quasi-mono-energetic neutron-induced fission of ^{238}U

H. Naik [a,*], Sadhana Mukerji [b], Rita Crasta [c], S.V. Suryanarayana [d], S.C. Sharma [d], A. Goswami [a]

[a] *Radiochemistry Division, Bhabha Atomic Research Centre, Mumbai 400 085, India*
[b] *Reactor Physics Design Division, Bhabha Atomic Research Centre, Mumbai 400 085, India*
[c] *Microtron Centre, Department of Studies in Physics, Mangalore University, Mangalagangotri 574 199, Karnataka, India*
[d] *Nuclear Physics Division, Bhabha Atomic Research Centre, Mumbai 400 085, India*

Abstract

The cumulative yields of various fission products in the 6.35, 8.53, 9.35 and 12.52 MeV quasi-mono-energetic neutron induced fission of ^{238}U have been determined by using the off-line γ-ray spectrometric technique. The mass chain yields were obtained from the fission product yields by using charge distribution correction. From the mass yield data, the peak-to-valley (P/V) ratio, the average value of light mass ($\langle A_L \rangle$), heavy mass ($\langle A_H \rangle$) and thus the average number of neutrons ($\langle \upsilon \rangle_{\text{expt}}$) were obtained in the ^{238}U(n, f) reaction for the above mentioned four neutron energies. The present and literature data in the ^{238}U(n, f) and ^{238}U (γ, f) reactions at various energies were compared to arrive at the following conclusions. (i) The yields of fission products for $A = 133$–134, $A = 138$–140, and $A = 143$–144 and their complementary products in the ^{238}U(n, f) and ^{238}U(γ, f) reactions are higher than other fission products, which has been explained from the point of even–odd effect and standard I and standard II asymmetric mode of fission. (ii) The yields of symmetric products increase and thus the peak-to-valley (P/V) ratios decrease with excitation energy, whereas the $\langle \upsilon \rangle_{\text{expt}}$ values increase with excitation energy. (iii) The variation of $\langle A_L \rangle$, $\langle A_H \rangle$ and $\langle \upsilon \rangle_{\text{expt}}$ values with excitation energy behave differently in between ^{238}U(n, f) and ^{238}U(γ, f) reactions, which may be due to the different types of reaction mechanism for the neutron and photon with ^{238}U.

---

* Corresponding author.
  E-mail address: naikhbarc@yahoo.com (H. Naik).

1. Introduction

The fission yield data in the low energy neutron induced fission of actinides are needed for decay heat calculation [1] and thus are important for reactor applications. In particular, the fission yield data in the neutron induced fission of ^{235}U, ^{238}U and ^{239}Pu has tremendous application in conventional (LWR, HWR) and fast reactors [2,3]. Among these three actinides, ^{238}U is associated with ^{235}U in conventional reactor and with ^{239}Pu in fast reactor [2,3]. Thus the fission product yields in the neutron induced fission of ^{238}U at different neutron energies are important for both conventional and fast reactors. Besides the reactor application, the fission product yields through mass and charge yield distribution in the low energy neutron induced fission of ^{238}U provide important information about the effect of nuclear structure and dynamics of descent from saddle to scission point [4,5]. However, with increase of neutron energy, the effects of nuclear structure such as the even–odd effect decreases and thus the fine structure in the mass yield distribution decrease. In the neutron induced fission of ^{238}U, the compound nucleus mass increases by one unit, whereas in the photon induced fission, the mass and charge of the compound nucleus are the same as those of target nucleus. Thus the fission studies in neutron induced fission of ^{238}U in comparison with the photon induced fission give better understanding of nuclear physics.

Sufficient data on fission product yields relevant to mass yield distribution studies in the reactor neutron [6,7] and mono-energetic neutron [8–35] induced fission of ^{238}U are available in literature. Similarly, fission product yields in the neutron induced fission of lighter mass uranium isotopes (e.g. ^{232,233,235}U) at various energies are available in different compilations [36–41]. On the other hand, the fission product yields in the bremsstrahlung induced fission of ^{238}U are available in literature [42–63]. The yields of fission fragments in the excitation energy range of the GDR region due to electromagnetic fission in inverse kinematics [64–66] are available for neutron-deficient lighter mass uranium isotopes (e.g. $^{231–234}$U). From these data, it can be seen that in the neutron [8–35] and bremsstrahlung [42–63] induced fission of ^{238}U, the yields of fission products are higher around mass numbers 133–135, 138–140 and 143–145 and their complementary products [6,7]. This is due to nuclear structure effects such as the even–odd effect [67]. In the electromagnetic fission of lighter actinides [64–66], the higher yields of the fission products around mass numbers 133–135 corresponding to a most probable charge of 52 have been also observed. The higher yields of the fission products around mass number 133–135 and 143–145 is explainable from the point of the standard I and standard II asymmetric fission modes as mentioned by Brosa et al. [68] based shell effect [69]. However, from the above data, it is not clear at what neutron and photon energy the effect of nuclear structure disappears. In the case of photon induced fission of ^{238}U [42–66], most of the data are based on bremsstrahlung induced fission, where the low energy photons also contribute to the fission. Thus it is not possible to delineate at what energy the nuclear structure effect disappears. Besides this, comparison of the experimental fission product yields between the ^{238}U(n, f) and ^{238}U(γ, f) reactions show that the average light mass ($\langle A_L \rangle$) and heavy mass ($\langle A_H \rangle$) have different trend [63]. However,

fission product yields data are not available within the neutron energies of 11.3–14 MeV for the ^{238}U(n, f) reaction to examine the above aspect and nuclear structure effect. Most of the fission product yields in the ^{238}U(n, f) [8–35] based on off-line and γ-ray spectrometric technique are available within neutron energy of 1.5–11.3 MeV [24–26] and around 14 MeV [9–23,27–33]. Some data in the reactor neutron [6,7] and 3.72–10.09 MeV quasi-mono-energetic neutron [35] induced fission of ^{238}U are also determined by using off-line gamma ray spectrometric technique, where the nuclear structure was clearly shown. However, no fission product yields are available in literature for the ^{238}U(n, f) reaction within the neutron energies of 11.3 to 14 MeV. At higher energy, the experimental results are available in the 33–60 MeV quasi-mono-energetic neutron-induced fission of ^{238}U by using the physical measurement [34], where the effect of nuclear structure is not expected. It is even not possible to examine the nuclear structure effect from the data of physical measurement. This is because to obtain the fission product yields from the fragment yields needs neutron emission correction, which is not an easy task due to the unavailability of neutron emission curve. In view of this, in the present work, the yields of various fission products in 6.35, 8.53, 9.35 and 12.52 MeV quasi-mono-energetic neutron-induced fission of ^{238}U have been determined by using off-line γ-ray spectrometric technique. From the yields of the fission products, their mass chain yields were obtained by using charge distribution correction [37,70]. The fission product yields in the above four neutron energies of the present work and at other neutron energies from literature [8–35] in the ^{238}U(n, f) reaction are compared with the similar data in the ^{238}U(γ, f) reaction [42–63] to examine the role of excitation energy on the nuclear structure effect. The effect of excitation energy on peak-to-valley (P/V) ratio, average neutron numbed ($\langle \upsilon \rangle$), and average light mass ($\langle A_L \rangle$) and heavy mass ($\langle A_H \rangle$) have also been discussed.

2. Experimental details

The neutron beam was obtained from the ^{7}Li$(p, n)^7$Be reaction by using the proton beam from the 14UD BARC-TIFR Pelletron facility at Mumbai, India [71–73]. The main proton beam line at 6 m height above the analyzing magnet of the Pelletron facility was utilized to have a maximum proton current from the accelerator. At this port, the terminal voltage is regulated by generating voltage mode (GVM) using terminal potential stabilizer. A proton beam collimator of 6 mm diameter was used before the Li target to avoid the energy spread of the proton beam. The lithium foil used for the neutron production was made up of natural lithium with thickness of 3.7 mg/cm^2, sandwiched between two tantalum foils of different thickness. The front tantalum foil facing the proton beam is 3.9 mg/cm^2 thick, in which the degradation of the proton energy is only 50–80 keV [74]. On the other hand the back tantalum foil is 0.025–0.1 mm thick, which is sufficient to stop the proton beam. Behind the Ta–Li–Ta stack, the samples used for irradiation were placed. The samples for irradiation consist of natural ^{238}U metal foil sample wrapped with 0.025 mm thick 99.99% pure aluminum foil. Different sets of Ta–Li–Ta stacks and Al wrapped U samples were made for irradiations at various neutron energies. The aluminum wrapper was used as a catcher foil to stop fission products recoiling out from the ^{238}U metal foil during the irradiation. The sizes of the ^{238}U metal foils were 1.0 cm^2 in area with thickness of 344.1–634.2 mg/cm^2. The sample was mounted at zero degree angle in the forward direction with respect to the beam direction at a distance of 2.1 cm from the location of the Ta–Li–Ta stack. The sample was then irradiated with neutrons generated by impinging the proton beam on the lithium metal foil through the thin tantalum foil of the Ta–Li–Ta metal stack. The energies of proton beam used were 10, 14, 16 and 20 MeV, which correspond to the maximum neutron
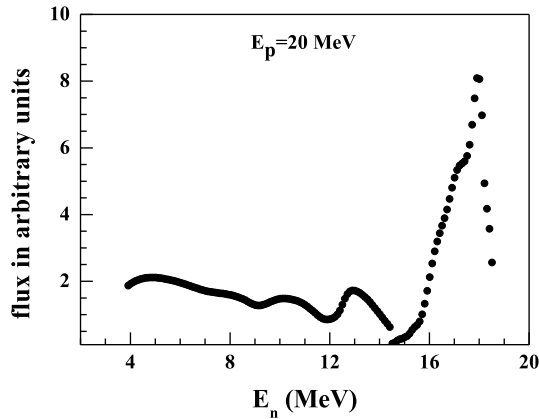
Fig. 1. Neutron spectrum from ^{7}Li(p, n) reaction for the proton energy of 20.0 MeV calculated using the results of Meadows and Smith [77].

energies of 8.12, 12.12, 14.12 and 18.12 MeV, respectively. The proton current during the irradiations varied from 200 to 400 nA. A typical neutron spectrum for proton energy of 20 MeV is shown in Fig. 1 as in the case of other proton energies [72,73].

The aluminum wrapped uranium samples were irradiated for 5–10 h depending upon the energy and current of the proton beam facing by the thin tantalum target. After irradiation, the samples were cooled for 1–2 h. The irradiated targets were mounted on different Perspex plates and taken for γ-ray counting. The γ-rays of fission products from the irradiated samples were counted in an energy and efficiency calibrated 80 cm^3 HPGe detector coupled to a PC-based 4 K channel analyzer. The counting dead time was kept always <5% by placing the irradiated sample at a suitable distance from the end cap of the detector to avoid pileup effects. The γ-ray counting of the sample was done in live time mode and was followed as a function of time. The resolution of the detector system during counting was 1.8 keV FWHM at 1332.5 keV of ^{60}Co. The energy and efficiency calibration of the detector system was performed with a standard ^{152}Eu source with γ-ray energies from 121.8 to 1408.01 keV. The γ-ray counting of the standard sources was done at the same geometry by keeping in mind the summation error. The detector efficiency was 20% at 1332.5 keV relative to 3″ diameter ×3″ length NaI(Tl) detector. The uncertainty in the detector efficiency was 2–3%. For each irradiated uranium samples, several sets of measurements were performed with increasing counting time to cover the fission products with different half-lives. This also helps to avoid the interfering γ-ray energies of different fission products. The γ-ray counting of the irradiated uranium samples was done for a few months to check the half-life of the fission products of interest. Since the cooling time of the irradiated samples was 1–2 h, it was possible to measure the fission products with half-lives of 30 min to 284 days.

3. Calculation and results

3.1. Calculation of the neutron energy and average excitation energy

The neutron flux in the present work was produced in the ^{7}Li(p, n) reaction of the natural lithium. However, in natural lithium, the isotopic abundances of ^{6}Li and ^{7}Li are 7.59% and 92.41%, respectively. Besides the ^{7}Li(p, n) reaction, the ^{6}Li(p, n) and ^{6}Li(p, pn) reactions also

takes place at higher neutron energy. The threshold energy of the ^{6}Li(p, n) and ^{6}Li(p, pn) reactions are 5.92 and 6.62 MeV, respectively. Thus the neutron yield contribution from the ^{6}Li(p, n) and ^{6}Li(p, pn) reactions are negligible below an incident proton energy of 9 MeV [75] due to its low isotopic abundance and higher threshold value. The Q-value for the ^{7}Li$(p, n)^7$Be reaction leading to the ground and first excited states are -1.644 and -2.079 MeV, respectively. Thus for the ^{7}Li$(p, n)^7$Be reaction, the average Q-value above the ground state is -1.868 MeV. The threshold value to populate the ground and first excited states of ^{7}Be are 1.881 and 2.37 MeV, respectively. Thus for the proton energies of 10, 14, 16 and 20 MeV, the resulting peak energies of the first group of neutrons (n_0), for the ground state of ^{7}Be will be 8.12, 12.12, 14.12 and 18.12 MeV, respectively. The corresponding neutron energies of the second group of neutrons (n_1), for the first excited state of ^{7}Be will be 7.63, 11.63, 13.63 and 17.63 MeV, respectively (Fig. 1). Above a proton energy of 4.5 MeV, the fragmentation of ^{8}Be to ^{4}He $+ ^3$He $+ n$ $(Q = -3.23$ MeV) takes place and other reaction channels open up, leading to a continuous neutron energy distribution besides the n_0 and n_1 groups of neutrons. Thus the neutron spectrum has the maximum flux peaking at first (n_0) and second (n_1) groups of neutrons and continuous low flux tailing part at lower energy (Fig. 1). The branching ratio to the ground state and first excited state of ^{7}Be up to $E_p = 7$ MeV is given by Liskien and Paulsen [76] as well as by Meadows and Smith [77]. Similarly, Poppe et al. [75] have given the branching ratio to the ground state and first excited state of ^{7}Be for $E_p = 4.2$ MeV to 26 MeV. On the other hand, Meadows and Smith [77] have given experimental neutron distributions from the break up channels and also parameterized these distributions. Based on those parameters, we have generated the neutron spectrum using the neutron energy distribution [75–77] and shown in our earlier work [72,73]. From those neutron spectra [72,73], the flux-weighted average neutron energies were calculated as 6.35, 8.53, 9.35 and 12.52 MeV corresponding to the proton energies of 10, 14, 16 and 20 MeV, respectively. The energy spread for the average neutron energies is around 0.3 to 0.7 MeV [72,73]. Using the average neutron energies, the average excitation energies for the compound nucleus ^{239}U* were calculated by using the following equation.

$$\langle E^*\rangle = \left[(\Delta m \text{ of } ^{238}\text{U} + \Delta m \text{ of } n) - \Delta m \text{ of } ^{239}\text{U}^*\right] + \langle E_n\rangle \tag{1}$$

The Δm values of the neutron, ^{238}U and ^{239}U are taken from the nuclear Wallet cards [78]. The average excitation energies obtained are 10.7, 12.88, 13.7 and 16.87 MeV corresponding to the average neutron energies given above.

3.2. Calculation of fission product yields

The number of detected γ-rays (N_{obs}) corresponding to the activity of fission products were obtained from their total peak areas by subtracting the linear Compton background. The number of detected γ-rays (N_{obs}) under the photo-peak of an individual fission product is related to the their cumulative yields (Y_c) with the decay equation [6,7] given below.

$$N_{\text{obs}}(T_{\text{CL}}/T_{\text{LT}}) = n\sigma_f \varphi Y_c I_\gamma \varepsilon \left(1 - e_{\text{irr}}^{-\lambda t}\right) e_{\text{cool}}^{-\lambda t} \left(1 - e^{-\lambda \text{CL}}\right)/\lambda \tag{2}$$

where n is the number of target atoms, φ is the neutron flux and σ_f is the ^{238}U(n, f) reaction cross-section at average neutron energies of 6.35, 8.53, 9.35 and 12.52 MeV. I_γ is the branching ratio or relative intensity of the γ ray, ε is the detection efficiency of the γ rays in the detector system and $\lambda = \ln 2/T_{1/2}$ is the decay constant of the fission-product with half-life $T_{1/2}$. t_{irr} and t_{cool} are the irradiation and cooling times, whereas, T_{CL} and T_{LT} are the real time and the live time of counting, respectively.

The cumulative yields (Y_c) of various fission products relative to ^{135}I were calculated from equation (2). The nuclear spectroscopic data, such as the γ-ray energies, the half-lives ($T_{1/2}$), and the γ-ray intensity (I_γ) of the fission products were taken from the literature [79,80]. From the relative cumulative yields (Y_C) of the fission products, their relative mass-chain yields (Y_A) were calculated by using Wahl's prescription of charge distribution [37]. According to this, the fractional cumulative yield (Y_{FCY}) of a fission product in an isobaric mass chain is given as

$$Y_{\mathrm{FCY}} = \frac{\mathrm{EOF}^{a(Z)}}{\sqrt{2\pi\sigma^2}} \int\limits_{-\infty}^{Z+0.5} \exp\left[-(Z - Z_P)^2/2\sigma^2\right] dZ \tag{3}$$

$$Y_A = Y_C / Y_{\mathrm{FCY}} \tag{4}$$

where Z_P is the most probable charge, σ_z is the width parameter and Y_A is the mass chain yield of an isobaric-yield distribution. $\mathrm{EOF}^{a(Z)}$ is the even–odd factor with $a(Z) = +1$ for even-Z nuclides and -1 for odd-Z nuclides.

It can be seen from the above equations that in an isobaric mass chain, for the calculation of Y_{FCY} and thus Y_A values of a fission product, it is necessary to have knowledge of Z_P, σ_z and $\mathrm{EOF}^{a(Z)}$. The $\mathrm{EOF}^{a(Z)}$ values in the medium energy fission are negligible. The σ_z value of 0.70 ± 0.06 in medium energy proton and alpha induced fission of ^{232}Th and ^{238}U was obtained by Umezawa et al. [70]. The Z_P values of individual mass chain (A) for the above fission systems were calculated by using the following equations [70]:

$$Z_P = \eta Z_F \pm \Delta Z_P, \quad \eta Z_F = Z_{\mathrm{UCD}} = (Z_F/A_F)(A + \upsilon_{\mathrm{post}}) \tag{5a}$$

$$\eta = (A + \upsilon_{\mathrm{post}})/(A_C - \upsilon_{\mathrm{pre}}), \qquad A_F = A_C - \upsilon_{\mathrm{pre}} \tag{5b}$$

where Z_C and A_C are the charge and mass of the compound nucleus. Z_F and A_F are the charge and mass of the fissioning system. Z_{UCD} is the most probable charge based on the unchanged charge-density distribution as suggested by Sugarman and Turkevich [81]. ΔZ_P ($= Z_P - Z_{\mathrm{UCD}}$) is the charge-polarization parameter. The $+$ and $-$ signs for the ΔZ_P value are applicable to light and heavy fragments, respectively. A is the mass of the fission product, whereas υ_{pre} and υ_{post} are pre- and post-fission neutrons, which can be calculated as [70]

$$\upsilon_{\mathrm{pre}} = \frac{\langle E^* \rangle}{7.5 \pm 0.5} + \frac{Z_C}{2A_C} - (19.0 \pm 0.5) \tag{6a}$$

$$\begin{aligned} \upsilon_{\mathrm{post}} &= 1.0 \quad \text{for } A > 88 \\ &= 1.0 + 0.1(A - 88) \quad \text{for } 78 < A < 88 \\ &= 0 \quad \text{for } A < 78 \end{aligned} \tag{6b}$$

The average excitation energies of 10.7, 12.88, 13.7 and 16.87 MeV corresponding to the average neutron energies of 6.35, 8.53, 9.35 and 12.52 MeV were used in Eq. (6a) to calculate the υ_{pre} values. The values of υ_{pre} and υ_{post} obtained based on Eqs. (6a) and (6b) were used in Eqs. (5a) and (5b) to calculate the value of Z_{UCD} as a function of mass number for the different fission products. The ΔZ_P value was then calculated by using the following relation [70]:

$$\Delta Z_P = 0 \quad \text{for } I\eta - 0.5I < 0.04 \tag{7a}$$

$$\Delta Z_P = (20/3)(I\eta - 0.5I - 0.04) \quad \text{for } 0.04 < I\eta - 0.5I < 0.085 \tag{7b}$$

The Z_P values as a function of mass number and the average width parameter (σ_z) of 0.7 were used in Eq. (3) to obtain the Y_{FCY} values for individual fission products. The mass-chain yield (Y_A) of the fission products from their relative cumulative yield (Y_C) was obtained from Eq. (4) by using the Y_{FCY} values of different fission products. The relative mass-chain yields of the fission products obtained were then normalized to a total yield of 200% to calculate the absolute mass-chain yields. The absolute cumulative yields of the fission products in the 6.35, 8.53, 9.35 and 12.52 MeV neutron-induced fission of ^{238}U were then obtained by using the mass-yield data and Y_{FCY} values. The relative cumulative yield (Y_C) and mass-chain yield (Y_A) of the fission products in the 6.35, 8.53, 9.35 and 12.53 MeV neutron-induced fission of ^{238}U along with the nuclear spectroscopic data from Refs. [79,80] are given in Tables 1–4. The absolute mass-chain yields in the ^{238}U(n, f) reaction from the present work for the above mentioned four neutron energies are also given in the last column of Tables 1–4.

The uncertainty shown in the cumulative yield of the individual fission products shown in Tables 1–4 is the statistical fluctuation from the replicate measurements. The overall uncertainty represents contributions from both statistical and systematic uncertainties. The statistical uncertainty in the number of detected γ-ray activity is estimated to be 5%–10%, which was determined by accumulating the data for the optimum period of time, depending on the half-life of fission products. The systematic uncertainties are due to the uncertainties in irradiation time (0.2%), detector efficiency calibration ($\sim$3%), half-life of the fission products ($\sim$1%), and γ-ray abundance ($\sim$2%), which is the largest variation in the literature [79,80]. Thus, the overall systematic uncertainty is about 3.8%. An upper limit of uncertainty of 6.3%–10.7% was estimated for the yields of fission-products based on 5%–10% statistical and a 3.8% systematic uncertainty.

4. Discussion

The fission products yields in the ^{238}U(n, f) reaction for quasi-mono-energetic neutron energies of 12.52 MeV shown in Table 4 are determined for the first time. On the other hand, the fission products yield data for the average neutron energies of 6.35, 8.53 and 9.35 MeV from the present work given in Tables 1–3 are in general agreement with the available literature data for the mono-energetic neutron of 6.0, 6.9, 8.1 and 9.1 MeV [24,25]. However, the literature data [24,25] are for purely mono-energetic neutrons based on ^{2}H(d, n) ^{3}He reaction, whereas the present data are for quasi-mono-energetic neutrons based on ^{7}Li(p, n) reaction. The mass-chain-yield data in the ^{238}U(n, f) reaction from the present work are plotted in Fig. 2 as a function of their mass number. In the same figure, the mass-chain yield data in the ^{238}U(γ, f) reaction with the end-point bremsstrahlung energies of 13.4, 17.3, 20 and 48 MeV [42,54,63] having comparable excitation energies were also plotted for comparison. It can be seen from Fig. 2 that in both the ^{238}U(n, f) and ^{238}U(γ, f) reactions, the yields of fission products for $A = 133$–134, 138–140 and 143–144 as well as their complementary products are higher than the other fission products. The oscillation of higher yields for the above heavy mass products and their complementary light mass products in the interval of five mass and two charge units in the ^{238}U(n, f) and ^{238}U(γ, f) reactions is due to the even–odd effect [61]. This is because the A/Z ratio of the fission products and fissioning system is around 2.5. Thus the difference of two charges makes the oscillation of mass yield in the interval of five mass units. It can also be seen from Fig. 2 that the amplitude of oscillation in the interval of five mass units is slightly lower in the 6.35–12.52 MeV neutron and 13.4–48 MeV bremsstrahlung induced fission of ^{238}U. This is in accordance with their even–odd effects [58,67], which is slightly lower in the fissioning system ^{238}U* [58] compared to ^{239}U* [67]. Besides the even–odd effect, the higher yields of fission

Table 1
Nuclear spectroscopic data and yields of fission products in the 6.35 MeV neutron-induced fission of ^{238}U.

Nuclide	Half-life	γ-ray energy (keV)	γ-ray abundance (%)	Y_C (%)	Y_A (%)
^{84}Br	31.8 min	1616.2	6.2	0.642 ± 0.044	0.643 ± 0.044
^{85}Kr^m	4.48 h	151.2	75.0	0.937 ± 0.042	0.937 ± 0.042
		304.9	14.0	0.932 ± 0.052	0.932 ± 0.052
^{87}Kr	76.3 min	402.6	49.6	1.680 ± 0.136	1.685 ± 0.137
^{88}Kr	2.84 h	196.3	25.9	2.063 ± 0.165	2.090 ± 0.167
^{91}Sr	9.63 h	749.8	23.6	3.352 ± 0.268	3.352 ± 0.268
		1024.3	33.0	3.419 ± 0.307	3.419 ± 0.307
^{92}Sr	2.71 h	1384.9	90.0	3.630 ± 0.253	3.634 ± 0.253
^{93}Y	10.18 h	266.9	7.3	3.301 ± 0.226	3.301 ± 0.226
^{95}Zr	64.02 d	756.7	54.0	5.324 ± 0.287	5.324 ± 0.287
		724.3	44.2	5.056 ± 0.307	5.056 ± 0.307
^{97}Zr	16.91 h	743.4	93.0	6.218 ± 0.353	6.224 ± 0.353
^{99}Mo	65.94 h	140.5	89.4	5.041 ± 0.258	5.041 ± 0.258
		739.5	12.13	5.733 ± 0.239	5.733 ± 0.239
^{103}Ru	39.26 d	497.1	90.0	5.962 ± 0.209	5.962 ± 0.209
^{105}Ru	4.44 h	724.4	47.0	3.370 ± 0.232	3.390 ± 0.234
^{105}Rh	35.36 h	319.1	19.2	3.429 ± 0.214	3.429 ± 0.214
^{112}Ag	3.13 h	617.5	43.0	0.307 ± 0.078	0.307 ± 0.078
^{113}Ag	5.37 h	298.6	10.0	0.221 ± 0.024	0.221 ± 0.024
^{115}Cd^g	53.46 h	336.2	45.9	0.122 ± 0.019	
^{115}Cd^{total}				0.143 ± 0.019[a]	0.143 ± 0.019[a]
^{117}Cd^m	3.36 h	1066.0	23.1	0.033 ± 0.009	
		1097.3	26.0	0.037 ± 0.009	
^{117}Cd^g	2.49 h	273.4	28.0	0.099 ± 0.014	
^{117}Cd^{total}				0.134 ± 0.014	0.134 ± 0.014
^{127}Sb	3.85 d	687.0	37.0	0.594 ± 0.078	0.594 ± 0.078
^{128}Sn	59.07 min	482.3	59.0	0.780 ± 0.056	0.818 ± 0.058
^{129}Sb	4.32 h	812.4	43.0	1.315 ± 0.107	1.320 ± 0.107
^{131}I	8.02 d	364.5	81.7	2.840 ± 0.239	2.840 ± 0.239
^{132}Te	3.2 d	228.1	88.0	5.341 ± 0.320	5.368 ± 0.321
^{133}I	20.8 h	529.9	87.0	6.337 ± 0.309	6.337 ± 0.309
^{134}Te	41.8 min	566.0	18.0	7.004 ± 0.351	7.556 ± 0.378
		767.2	29.5	6.841 ± 0.357	7.380 ± 0.385
^{134}I	52.5 m	847.03	95.9	7.715 ± 0.323	7.730 ± 0.223
		884.09	65.0	7.836 ± 0.333	7.836 ± 0.333
^{135}I	6.57 h	1131.5	22.7	5.509 ± 0.305	5.548 ± 0.307
		1260.4	28.9	5.427 ± 0.285	5.465 ± 0.287
^{138}Cs^g	33.41 min	1435.8	76.3	6.615 ± 0.331	6.615 ± 0.331
		1009.8	29.8	7.078 ± 0.346	7.078 ± 0.346
		462.8	30.7	7.112 ± 0.356	7.112 ± 0.356
^{139}Ba	83.03 min	165.8	23.7	7.107 ± 0.273	7.107 ± 0.273
^{140}Ba	12.75 d	537.3	24.4	6.561 ± 0.214	6.561 ± 0.214
^{141}Ce	32.5 d	145.4	48.0	5.967 ± 0.209	5.967 ± 0.209
^{142}La	91.1 min	641.3	47.0	4.559 ± 0.273	4.559 ± 0.273
^{143}Ce	33.03 h	293.3	42.8	4.983 ± 0.297	4.983 ± 0.297
^{144}Ce	284.89 d	133.5	11.09	5.188 ± 0.351	5.188 ± 0.351
^{147}Nd	10.98 d	531.0	13.1	3.663 ± 0.217	3.663 ± 0.217
^{149}Nd	1.728 h	211.3	25.9	2.307 ± 0.155	2.316 ± 0.156
		270.2	10.6	2.226 ± 0.108	2.226 ± 0.108
^{151}Pm	53.08 h	340.8	23.0	1.166 ± 0.103	1.168 ± 0.104
^{153}Sm	46.28 h	103.2	30.0	0.439 ± 0.029	0.439 ± 0.032

Y_C – Cumulative yields, Y_A – Mass yields, ^{135}I – Fission rate monitor.
  [a] The yields of ^{115}Cd^{total} is based on the ratio of ^{115}Cd^g/^{115}Cd^m = 6 from Ref. [25].

Table 2

Nuclear spectroscopic data and yields of fission products in the 8.53 MeV neutron-induced fission of ^{238}U.

Nuclide	Half-life	γ-ray energy (keV)	γ-ray abundance (%)	Y_C (%)	Y_A (%)
^{84}Br	31.8 min	1616.2	6.2	0.641 ± 0.038	0.642 ± 0.038
^{85}Kr^m	4.48 h	151.2	75.0	0.954 ± 0.042	0.954 ± 0.042
		304.9	14.0	0.963 ± 0.056	0.963 ± 0.056
^{87}Kr	76.3 min	402.6	49.6	1.614 ± 0.153	1.619 ± 0.153
^{88}Kr	2.84 h	196.3	25.9	2.199 ± 0.142	2.228 ± 0.144
^{91}Sr	9.63 h	749.8	23.6	3.763 ± 0.265	3.763 ± 0.265
		1024.3	33.0	3.647 ± 0.172	3.647 ± 0.172
^{92}Sr	2.71 h	1384.9	90.0	3.915 ± 0.312	3.919 ± 0.312
^{93}Y	10.18 h	266.9	7.3	3.766 ± 0.360	3.766 ± 0.360
^{95}Zr	64.02 d	756.7	54.0	4.731 ± 0.283	4.731 ± 0.283
		724.3	44.2	5.077 ± 0.274	5.077 ± 0.274
^{97}Zr	16.91 h	743.4	93.0	6.170 ± 0.345	6.177 ± 0.346
^{99}Mo	65.94 h	140.5	89.4	5.202 ± 0.125	5.202 ± 0.125
		739.5	12.13	5.547 ± 0.139	5.547 ± 0.139
^{103}Ru	39.26 d	497.1	90.0	5.278 ± 0.221	5.278 ± 0.221
^{105}Ru	4.44 h	724.4	47.0	3.423 ± 0.234	3.444 ± 0.235
^{105}Rh	35.36 h	319.1	19.2	3.497 ± 0.245	3.497 ± 0.245
^{112}Ag	3.13 h	617.5	43.0	0.389 ± 0.034	0.389 ± 0.034
^{113}Ag	5.37 h	298.6	10.0	0.330 ± 0.028	0.330 ± 0.028
^{115}Cd^g	53.46 h	336.2	45.9	0.214 ± 0.033	
^{115}Cd^{total}				0.247 ± 0.033[a]	0.247 ± 0.033[a]
^{117}Cd^m	3.36 h	1066.0	23.1	0.065 ± 0.014	
		1097.3	26.0	0.056 ± 0.014	
^{117}Cd^g	2.49 h	273.4	28.0	0.177 ± 0.023	
^{117}Cd^{total}				0.237 ± 0.028	0.237 ± 0.028
^{127}Sb	3.85 d	687.0	37.0	0.777 ± 0.072	0.778 ± 0.072
^{128}Sn	59.07 min	482.3	59.0	1.077 ± 0.087	1.129 ± 0.091
^{129}Sb	4.32 h	812.4	43.0	1.713 ± 0.153	1.719 ± 0.154
^{131}I	8.02 d	364.5	81.7	2.949 ± 0.341	2.949 ± 0.341
^{132}Te	3.2 d	228.1	88.0	5.085 ± 0.354	5.111 ± 0.355
^{133}I	20.8 h	529.9	87.0	6.340 ± 0.235	6.340 ± 0.235
^{134}Te	41.8 min	566.0	18.0	6.844 ± 0.343	7.375 ± 0.370
		767.2	29.5	7.093 ± 0.352	7.644 ± 0.379
^{134}I	52.5 m	847.03	95.9	7.444 ± 0.312	7.459 ± 0.312
		884.09	65.0	7.459 ± 0.254	7.473 ± 0.255
^{135}I	6.57 h	1131.5	22.7	5.327 ± 0.176	5.365 ± 0.178
		1260.4	20.3	5.294 ± 0.243	5.331 ± 0.245
^{138}Cs^g	33.41 min	1435.8	76.3	5.658 ± 0.283	5.658 ± 0.283
		1009.8	29.8	5.879 ± 0.293	5.879 ± 0.293
		462.8	30.7	6.071 ± 0.303	6.071 ± 0.303
^{139}Ba	83.03 min	165.8	23.7	6.426 ± 0.293	6.426 ± 0.293
^{140}Ba	12.75 d	537.3	35.4	6.042 ± 0.216	6.042 ± 0.216
^{141}Ce	32.5 d	145.4	20.5	5.317 ± 0.235	5.317 ± 0.235
^{142}La	91.1 min	641.3	47.0	4.385 ± 0.173	4.385 ± 0.173
^{143}Ce	33.03 h	293.3	42.8	4.635 ± 0.202	4.635 ± 0.202
^{144}Ce	284.89 d	133.5	11.09	5.086 ± 0.211	5.086 ± 0.211
^{147}Nd	10.98 d	531.0	13.1	3.751 ± 0.183	3.751 ± 0.183
^{149}Nd	1.728 h	211.3	25.9	2.229 ± 0.201	2.238 ± 0.202
		270.2	10.6	2.291 ± 0.120	2.301 ± 0.120
^{151}Pm	53.08 h	340.8	23.0	1.166 ± 0.098	1.168 ± 0.098
^{153}Sm	46.28 h	103.2	30.0	0.394 ± 0.031	0.434 ± 0.034

Y_C – Cumulative yields, Y_A – Mass yields, ^{135}I – Fission rate monitor.

[a] The yields of ^{115}Cd^{total} is based on the ratio of ^{115}Cd^g/^{115}Cd^m = 6 from Ref. [25].

Table 3

Nuclear spectroscopic data and yields of fission products in the 9.35 MeV neutron-induced fission of ^{238}U.

Nuclide	Half-life	γ-ray energy (keV)	γ-ray abundance (%)	Y_C (%)	Y_A (%)
^{84}Br	31.8 min	1616.2	6.2	0.664 ± 0.042	0.665 ± 0.042
^{85}Kr^m	4.48 h	151.2	75.0	1.067 ± 0.062	1.067 ± 0.062
		304.9	14.0	1.076 ± 0.085	1.076 ± 0.085
^{87}Kr	76.3 min	402.6	49.6	1.962 ± 0.120	1.968 ± 0.121
^{88}Kr	2.84 h	196.3	25.9	2.361 ± 0.150	2.392 ± 0.152
^{91}Sr	9.63 h	749.8	23.6	3.898 ± 0.282	3.898 ± 0.282
		1024.3	33.0	3.699 ± 0.249	3.699 ± 0.249
^{92}Sr	2.71 h	1384.9	90.0	4.318 ± 0.254	4.322 ± 0.254
^{93}Y	10.18 h	266.9	7.3	3.898 ± 0.272	3.898 ± 0.272
^{95}Zr	64.02 d	756.7	54.0	4.733 ± 0.194	4.733 ± 0.194
		724.3	44.2	5.380 ± 0.240	5.380 ± 0.240
^{97}Zr	16.91 h	743.4	93.0	6.191 ± 0.203	6.197 ± 0.203
^{99}Mo	65.94 h	140.5	89.4	5.226 ± 0.152	5.226 ± 0.152
		739.5	12.13	5.449 ± 0.245	5.449 ± 0.245
^{103}Ru	39.26 d	497.1	90.0	5.763 ± 0.254	5.763 ± 0.254
^{105}Ru	4.44 h	724.4	47.0	3.401 ± 0.290	3.408 ± 0.291
^{105}Rh	35.36 h	319.1	19.2	3.496 ± 0.245	3.496 ± 0.245
^{112}Ag	3.13 h	617.5	43.0	0.439 ± 0.051	0.439 ± 0.051
^{113}Ag	5.37 h	298.6	10.0	0.328 ± 0.032	0.328 ± 0.032
^{115}Cd^g	53.46 h	336.2	45.9	0.237 ± 0.027	
^{115}Cd^{total}				0.277 ± 0.027[a]	0.277 ± 0.027[a]
^{117}Cd^m	3.36 h	1066.0	23.1	0.065 ± 0.009	
		1097.3	26.0	0.074 ± 0.014	
^{117}Cd^g	2.49 h	273.4	28.0	0.196 ± 0.031	
^{117}Cd^{total}				0.267 ± 0.036	0.267 ± 0.036
^{127}Sb	3.85 d	687.0	37.0	0.780 ± 0.065	0.780 ± 0.065
^{128}Sn	59.07 min	482.3	59.0	1.123 ± 0.079	1.178 ± 0.083
^{129}Sb	4.32 h	812.4	43.0	1.421 ± 0.083	1.427 ± 0.083
^{131}I	8.02 d	364.5	81.7	3.177 ± 0.222	3.177 ± 0.222
^{132}Te	3.2 d	228.1	88.0	4.765 ± 0.285	4.789 ± 0.286
^{133}I	20.8 h	529.9	87.0	6.174 ± 0.240	6.174 ± 0.240
^{134}Te	41.8 min	566.0	18.0	6.401 ± 0.192	6.890 ± 0.212
		767.2	29.5	6.727 ± 0.232	7.241 ± 0.249
^{134}I	52.5 m	847.03	95.9	7.107 ± 0.249	7.121 ± 0.249
		884.09	65.0	6.876 ± 0.207	6.890 ± 0.208
^{135}I	6.57 h	1131.5	22.7	5.397 ± 0.252	5.435 ± 0.254
		1260.4	28.9	5.150 ± 0.206	5.186 ± 0.208
^{138}Cs^g	33.41 min	1435.8	76.3	5.833 ± 0.291	5.833 ± 0.291
		1009.8	29.8	5.620 ± 0.282	5.620 ± 0.282
		462.8	30.7	5.990 ± 0.301	5.990 ± 0.301
^{139}Ba	83.03 min	165.8	23.7	5.990 ± 0.222	5.990 ± 0.222
^{140}Ba	12.75 d	537.3	24.4	5.768 ± 0.199	5.768 ± 0.199
^{141}Ce	32.5 d	145.4	48.0	5.348 ± 0.208	5.348 ± 0.208
^{142}La	91.1 min	641.3	47.0	4.909 ± 0.157	4.909 ± 0.157
^{143}Ce	33.03 h	293.3	42.8	5.283 ± 0.203	5.283 ± 0.203
^{144}Ce	284.89 d	133.5	11.09	5.426 ± 0.217	5.426 ± 0.217
^{147}Nd	10.98 d	531.0	13.1	3.376 ± 0.236	3.376 ± 0.236
^{149}Nd	1.728 h	211.3	25.9	2.240 ± 0.129	2.249 ± 0.129
		270.2	10.6	2.343 ± 0.102	2.352 ± 0.103
^{151}Pm	53.08 h	340.8	23.0	1.201 ± 0.129	1.206 ± 0.129
^{153}Sm	46.28 h	103.2	30.0	0.418 ± 0.038	0.460 ± 0.041

Y_R – Cumulative yields, Y_A – Mass yields, ^{135}I – Fission rate monitor.

[a] The yields of ^{115}Cd^{total} is based on the ratio of ^{115}Cd$^g/^{115}$Cd^m = 6 from Ref. [25].

Table 4
Nuclear spectroscopic data and yields of fission products in the 12.52 MeV neutron-induced fission of ^{238}U.

Nuclide	Half-life	γ-ray energy (keV)	γ-ray abundance (%)	Y_C (%)	Y_A (%)
^{84}Br	31.8 min	1616.2	6.2	0.695 ± 0.041	0.696 ± 0.041
^{85}Kr^m	4.48 h	151.2	75.0	1.171 ± 0.095	1.171 ± 0.095
		304.9	14.0	1.192 ± 0.095	1.192 ± 0.095
^{87}Kr	76.3 min	402.6	49.6	2.191 ± 0.108	2.195 ± 0.108
^{88}Kr	2.84 h	196.3	25.9	2.788 ± 0.145	2.822 ± 0.147
^{91}Sr	9.63 h	749.8	23.6	3.451 ± 0.211	3.451 ± 0.211
		1024.3	33.0	3.836 ± 0.153	3.836 ± 0.153
^{92}Sr	2.71 h	1384.9	90.0	4.312 ± 0.211	4.316 ± 0.211
^{93}Y	10.18 h	266.9	7.3	3.702 ± 0.162	3.701 ± 0.162
^{95}Zr	64.02 d	756.7	54.0	5.057 ± 0.220	5.057 ± 0.220
		724.3	44.2	5.290 ± 0.197	5.290 ± 0.197
^{97}Zr	16.91 h	743.4	93.0	5.899 ± 0.220	5.905 ± 0.220
^{99}Mo	65.94 h	140.5	89.4	4.644 ± 0.188	4.644 ± 0.188
		739.5	12.13	5.106 ± 0.260	5.106 ± 0.260
^{103}Ru	39.26 d	497.1	90.0	5.842 ± 0.184	5.842 ± 0.184
^{105}Ru	4.44 h	724.4	47.0	3.309 ± 0.206	3.316 ± 0.206
^{105}Rh	35.36 h	319.1	19.2	3.486 ± 0.242	3.486 ± 0.242
^{112}Ag	3.13 h	617.5	43.0	0.615 ± 0.049	0.615 ± 0.049
^{113}Ag	5.37 h	298.6	10.0	0.524 ± 0.040	0.525 ± 0.040
^{115}Cd^g	53.46 h	336.2	45.9	0.431 ± 0.039	
^{115}Cd^{total}				0.503 ± 0.039^a	0.503 ± 0.039^a
^{117}Cd^m	3.36 h	1066.0	23.1	0.126 ± 0.013	
		1097.3	26.0	0.117 ± 0.018	
^{117}Cd^g	2.49 h	273.4	28.0	0.354 ± 0.031	
^{117}Cd^{total}				0.476 ± 0.036	0.476 ± 0.036
^{127}Sb	3.85 d	687.0	37.0	0.843 ± 0.067	0.844 ± 0.067
^{128}Sn	59.07 min	482.3	59.0	1.251 ± 0.099	1.310 ± 0.099
^{129}Sb	4.32 h	812.4	43.0	1.667 ± 0.197	1.674 ± 0.197
^{131}I	8.02 d	364.5	81.7	3.639 ± 0.265	3.639 ± 0.265
^{132}Te	3.2 d	228.1	88.0	4.853 ± 0.254	4.877 ± 0.256
^{133}I	20.8 h	529.9	87.0	5.748 ± 0.193	5.748 ± 0.193
^{134}Te	41.8 min	566.0	18.0	6.005 ± 0.271	6.457 ± 0.288
		767.2	29.5	6.247 ± 0.225	6.717 ± 0.242
^{134}I	52.5 m	847.03	95.9	6.950 ± 0.219	6.964 ± 0.220
		884.09	65.0	6.704 ± 0.215	6.717 ± 0.215
^{135}I	6.57 h	1131.5	22.7	5.062 ± 0.209	5.097 ± 0.211
		1260.4	28.9	4.946 ± 0.203	4.981 ± 0.206
^{138}Cs^g	33.41 min	1435.8	76.3	5.465 ± 0.238	5.465 ± 0.238
		1009.8	29.8	6.246 ± 0.197	6.246 ± 0.197
		462.8	30.7	6.084 ± 0.188	6.084 ± 0.188
^{139}Ba	83.03 min	165.8	23.7	5.788 ± 0.238	5.788 ± 0.238
^{140}Ba	12.75 d	537.3	24.4	5.568 ± 0.197	5.568 ± 0.197
^{141}Ce	32.5 d	145.4	48.0	5.120 ± 0.220	5.120 ± 0.220
^{142}La	91.1 min	641.3	47.0	4.631 ± 0.188	4.631 ± 0.188
^{143}Ce	33.03 h	293.3	42.8	4.918 ± 0.206	4.918 ± 0.206
^{144}Ce	284.89 d	133.5	11.09	5.079 ± 0.242	5.079 ± 0.242
^{147}Nd	10.98 d	531.0	13.1	3.101 ± 0.157	3.101 ± 0.157
^{149}Nd	1.728 h	211.3	25.9	2.114 ± 0.170	2.118 ± 0.171
		270.2	10.6	2.117 ± 0.207	2.126 ± 0.207
^{151}Pm	53.08 h	340.8	23.0	1.185 ± 0.052	1.188 ± 0.052
^{153}Sm	46.28 h	103.2	30.0	0.382 ± 0.028	0.422 ± 0.031

Y_C – Cumulative yields, Y_A – Mass yields, ^{135}I – Fission rate monitor.
  a The yields of ^{115}Cd^{total} is based on the ratio of ^{115}Cd^g/^{115}Cd^m = 6 from Ref. [25].
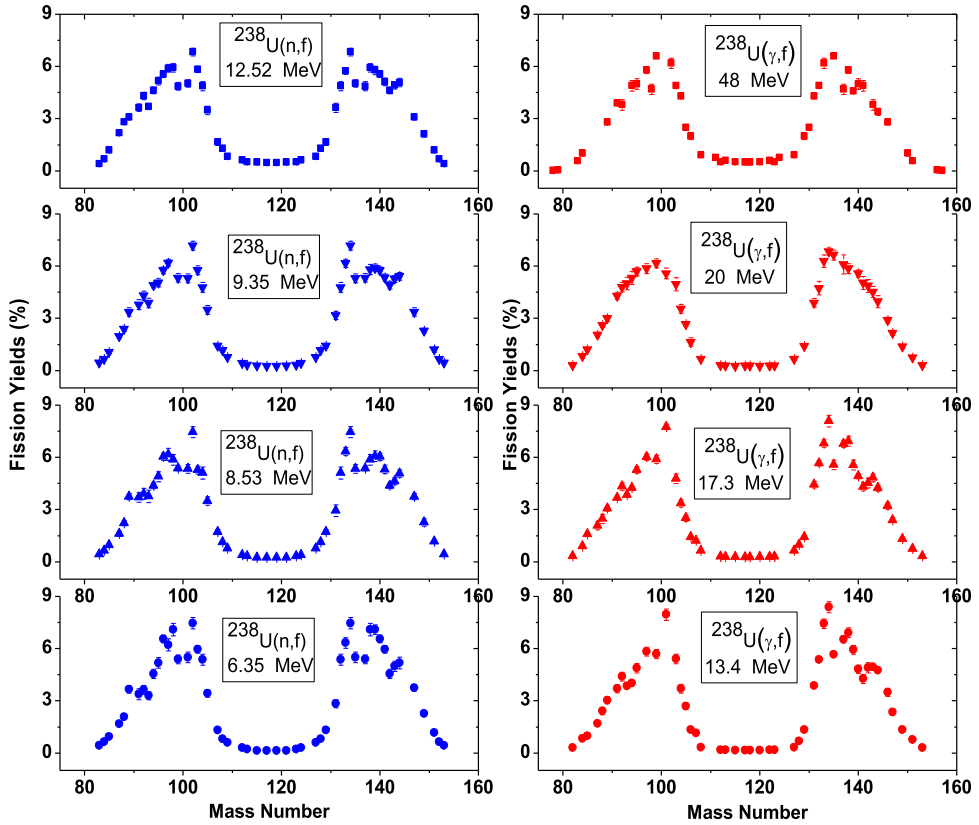
Fig. 2. Plot of mass yield distributions in the 6.35–12.52 MeV quasi-mono-energetic neutrons and 13.4–48.0 MeV bremsstrahlung-induced fission of ^{238}U.

products for $A = 133$–134, 138–140 and 143–144 can also be explained from the point of shell effect. However, the even–odd effect is out of phase with shell effect [69] and decreases with excitation energy [58]. For the fission products of $A = 133$–134, the corresponding fragments mass will be 134–135 based on one neutron emission. Then the most probable proton number is around 52 for the fragments mass of 134–135, which correspond to the most probable neutron number of 82–83. Thus the higher yields of the fission products for $A = 133$–134 is due to the presence of spherical $82n$ shell effect [69] in the corresponding fragment based on the standard I asymmetric mode of fission as mentioned by Brosa et al. [68]. Similarly, for the fission products of $A = 138$–140, the corresponding fragments mass will be 140–142 based on two neutrons emission. Then the most probable proton number is 54 for the fragment mass of 140–142, which correspond to the most probable neutron number of 86–88. Thus the higher yields of the fission products for $A = 138$–140 is due to presence of deformed 86–$88n$ shell [69] in the corresponding fragments based on the standard II asymmetric fission mode of fission [68]. For the fission products of $A = 143$–144, the corresponding fragment mass will be 145–146 based on two neutrons emission. Then the most probable proton number for fragment mass of 145–146 is around 56, which correspond to the most probable neutron number of 89–90. This is slightly higher than the deformed 86–$88n$ shell and thus the yields are not as high as in the case of the mass numbers of 133–134 and 138–140. Similar observation was made in our earlier work in
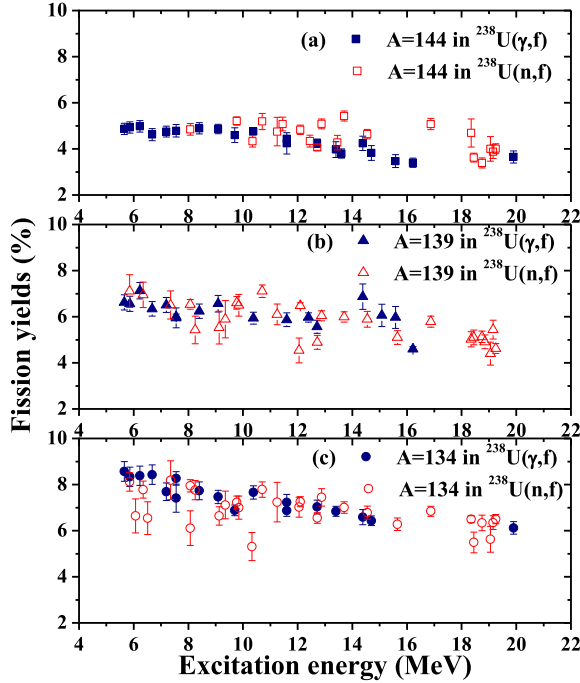
Fig. 3. Plot of yields of fission products (%) as a function of excitation energy for $A = 134$, 139 and 144 in the ^{238}U(n, f) and ^{238}U(γ, f) reactions.

the 3.72, 5.42, 7.75 and 10.09 MeV quasi-mono-energetic neutron [63] and 11.5, 13.4, 15.0 and 17.3 MeV bremsstrahlung [63] induced fission of ^{238}U. Same observation can be made from the fission products yields data in the 1.72–9.1 MeV neutron [24,25,29] and 6.12–70 MeV [54–60] bremsstrahlung induced fission of ^{238}U. The above observations support the even–odd effect and confirms the standard I and standard II asymmetric mode of fission based on spherical 82n and deformed 86–88n shell effect as mentioned by Brosa et al. [68]. However, it seems that the standard II asymmetric mode of fission is dominating for the fission products mass of 138–140, instead of 143–144.

Further, it can be seen from Fig. 2 that in the ^{238}U(n, f) and ^{238}U(γ, f) reactions, the yields of fission products for $A = 133$–134 are higher than for $A = 138$–140, which is in turn higher than for $A = 143$–144. In order to examine these aspects, the yields of fission products for $A = 134$, 139 and 144 from the present work and literature data in the ^{238}U(n, f) reaction [8–35] and in the ^{238}U(γ, f) reaction [42–63] are plotted in Fig. 3 as a function of excitation energy. It can be seen from Fig. 3 that the yields of fission products are ~7–9% for $A = 134$, ~7% for $A = 139$, ~5% for $A = 144$ and are comparable in both the ^{238}U(n, f) and ^{238}U(γ, f) reactions. For $A = 134$, the higher yield of ~8–9% in the ^{238}U(γ, f) reaction and ~7–8% in the ^{238}U(n, f) reaction cannot be explained based on the standard I and standard II asymmetric fission modes, unless the shell combinations of the complementary fragments are considered. As mentioned before, in both the ^{238}U(n, f) and ^{238}U(γ, f) reactions, the fission products for $A = 134$ and 139 have the spherical 82n and deformed 86–88n shell, if one and two neutron emissions are considered. However, the complementary fragment for $A = 134$ in the ^{238}U(n, f) and ^{238}U(γ, f) reactions, have the deformed 64–63n shell. Thus the highest yield for $A = 134$ and its complementary

product in the ^{238}U(n, f) and ^{238}U(γ, f) reactions are due to the presence of spherical $82n$ and deformed 64–$63n$ shell combination. Similarly, the complementary fragment for $A = 139$ in the ^{238}U(n, f) and ^{238}U(γ, f) reactions have the deformed $38p$ and $62n$ shell. Thus the higher yield for $A = 139$ and its complementary product is due to the presence of deformed $86n$ and $38p/62n$ shell combinations. Besides the shell combination, the higher yield for $A = 133$–134 and 138–140 in the ^{238}U(γ, f) and ^{238}U(n, f) reactions with most probable Z of 52 and 54 are also favourable from the N/Z ratio between complementary fragments. The fissioning systems ^{238}U* and ^{239}U* have the N/Z ratios of 1.587 and 1.598, respectively. The fission fragments mass of 135, 140 and 146 corresponding to product masses of 134, 139 and 144 have the N/Z ratios around 1.577, 1.593 and 1.607, respectively. These values are based on the most probable neutron-to-proton ratios of 82/52, 86/54 and 90/56, respectively. Thus the higher yields for $A = 133$–134 and 138–140 in the ^{238}U(γ, f) and ^{238}U(n, f) reactions are due to the favourable N/Z ratios of the corresponding fragments besides the presence of the deformed $82n$ and $64n$ or $86n$ and $38p/62n$ shells combinations. For the fission products of $A = 143$–144, the N/Z value of 1.607 is slightly higher than the value of 1.587 and 1.598 for the fission systems of ^{238}U* and ^{239}U*. Although, the fission products with $A = 143$–144 approach the deformed $88n$ shell closure, their complementary products are far from any proton or neutron shell closure in their fragments stage. So the yield of fission products for $A = 143$–144 and their complementary products are lower than those of the fission products with $A = 133$–134, 138–140 and their complementary products but higher than other fission products. Once the fission products for $A = 143$–144 and their complementary have the shell combinations, high fission products yields can be expected. As an example in ^{229}Th(n, f) reaction [82,83], the fission products for $A = 144$ and its complementary products for $A = 84$ have the highest fission yields of 10.85% due to the presence of deformed $88n$ and spherical $50n$ shell combination. These observations indicate that the fission product and its complementary product have the highest yield if both complementary fragments pairs have the neutron and/or proton shell combinations. If one of the fragment of the complementary pairs has a closed neutron or proton shell then the yields are higher. If none of the fragments of the complementary pairs have a closed neutron or proton shell then the yields are the lowest.

It can be also seen from Fig. 3 that the yields of fission products for $A = 134$, 139 and 144 in the ^{238}U(n, f) and ^{238}U(γ, f) reactions decrease with excitation energy. The decrease trend of fission products yields for $A = 134$ is slightly sharper in the ^{238}U(γ, f) reaction than in the ^{238}U(n, f) reaction. In order to examine the role of excitation energy, the yield of symmetric products, high yield asymmetric products and the peak-to valley (P/V) ratios from the present work and literature data [8–35] in the ^{238}U(n, f) reaction are shown in Table 5. The yields from Table 5 and literature data [41–62] in the ^{238}U(γ, f) reaction are plotted in Fig. 4 as a function of excitation energy. In both the ^{238}U(n, f) and ^{238}U(γ, f) reactions, the yield of high-yield asymmetric product is for $A = 133$ or 134 and low yield symmetric product is for $A = 115$ or 117, depending upon the availability literature data. The P/V ratios from Table 5 in the ^{238}U(n, f) reaction and literature data [42–63] in the ^{238}U(γ, f) reaction are plotted in Fig. 5 as a function of excitation energy. It can be seen from Fig. 4 that in both the ^{238}U(n, f) and ^{238}U(γ, f) reactions, the yield of asymmetric products decrease slightly, whereas the yields of symmetric products increase significantly with excitation energy. This is to conserve the mass yield distribution of 200%. Fig. 4 also shows that the yield of symmetric products in the ^{238}U(n, f) reaction increase sharply up to excitation energy of 18 MeV and thereafter remains almost constant. However, in the ^{238}U(γ, f) reaction, the yields of symmetric products increases sharply up to the excitation energy of 15 MeV and thereafter remain almost constant. Accordingly, the peak-to-valley ratio in

Table 5
Yields of asymmetric (Y_a) and symmetric (Y_s) products and P/V ratio in neutron-induced fission of ^{238}U.

E_n (MeV)	E^* (MeV)	Y_a (%)	Y_s (%)	P/V ratio	Ref.
1.5	5.85	8.120 ± 0.400	0.0102 ± 0.0014	796.1 ± 116.1	[25]
1.5	5.85	–	0.0075 ± 0.0008	825.0	[10]
1.72	6.07	7.830 ± 0.930	–	–	[29]
2.0	6.35	7.780 ± 0.370	0.0121 ± 0.0017	643.0 ± 95.4	[25]
2.0	6.35	–	0.0135 ± 0.0014	452.0	[10]
2.16	6.55	7.510 ± 0.830	–	–	[29]
3.0	7.35	–	0.029 ± 0.003	238.0	[10]
3.0	7.35	8.190 ± 0.840	0.034 ± 0.006	240.9 ± 49.2	[20]
3.72	8.07	7.945 ± 0.267	0.038 ± 0.006	209.1 ± 33.7	[35]
3.72	8.07	7.490 ± 0.790	–	–	[29]
3.9	8.25	7.760 ± 0.420	0.034 ± 0.005	228.2 ± 35.8	[25]
3.9	8.25	–	0.047 ± 0.005	129.0	[10]
4.78	9.13	6.770 ± 0.700	–	–	[29]
4.8	9.15	–	0.068 ± 0.007	89.0	[10]
5.42	9.77	7.223 ± 0.277	0.074 ± 0.018	97.6 ± 24.1	[35]
5.5	9.85	7.000 ± 0.500	0.077 ± 0.011	90.9 ± 14.5	[25]
5.98	10.33	6.290 ± 0.800	–	–	[29]
6.0	10.35	6.132 ± 0.699	0.124 ± 0.010	49.5 ± 6.9	[24]
6.35	10.7	7.791 ± 0.434	0.134 ± 0.014	52.7 ± 6.9	[A]
6.9	11.25	7.240 ± 0.860	0.134 ± 0.018	54.0 ± 9.7	[25]
7.1	11.45	6.839 ± 0.595	0.121 ± 0.009	56.5 ± 6.5	[24]
7.7	12.05	7.020 ± 0.430	0.191 ± 0.032	36.8 ± 6.6	[25]
7.75	12.1	7.257 ± 0.215	0.202 ± 0.037	35.9 ± 6.7	[35]
8.1	12.45	6.713 ± 0.665	0.135 ± 0.011	49.7 ± 6.4	[24]
8.27	12.62	7.210 ± 0.430	0.227 ± 0.009	31.2 ± 1.6	[27]
8.53	12.88	7.466 ± 0.312	0.247 ± 0.033	29.3 ± 4.8	[A]
9.1	13.45	6.308 ± 0.688	0.191 ± 0.016	33.0 ± 4.5	[24]
9.35	13.7	7.006 ± 0.249	0.277 ± 0.027	24.5 ± 3.2	[A]
10.09	14.54	6.785 ± 0.286	0.338 ± 0.039	20.1 ± 2.5	[35]
11.3	15.65	6.660 ± 0.260	0.430 ± 0.050	15.5 ± 1.9	[30]
12.52	16.87	6.841 ± 0.220	0.503 ± 0.040	13.6 ± 1.4	[A]
13.0	17.35	–	0.570 ± 0.070	8.8	[10]
14.0	18.35	6.500 ± 0.150	0.860 ± 0.090	7.6 ± 0.8	[12]
14.0	18.35	–	0.970 ± 0.150	–	[22]
14.1	18.45	6.000 ± 0.210	0.950 ± 0.090	6.6 ± 0.6	[19]
14.4	18.75	6.340 ± 0.340	0.843 ± 0.048	7.5 ± 0.6	[23]
14.4	18.75	–	0.975 ± 0.055	–	[23]
14.7	19.05	6.360 ± 0.450	0.860 ± 0.090	7.4 ± 0.9	[15]
14.7	19.05	–	0.930 ± 0.120	–	[15]
14.8	19.15	6.350 ± 0.300	0.870 ± 0.150	7.3 ± 1.3	[21]
14.8	19.15	–	0.950 ± 0.070	–	[21]
14.9	19.25	6.50 ± 0.300	0.985 ± 0.039	6.6 ± 0.4	[28]
14.9	19.05	–	0.834 ± 0.039	–	[28]
15.0	19.35	–	0.780 ± 0.090	6.5	[10]
16.4	20.75	–	0.870 ± 0.100	5.8	[10]
17.7	22.05	–	0.740 ± 0.090	6.8	[10]

A – Present work.

Fig. 5 decreases up to 18 MeV in the ^{238}U(n, f) reaction and 15 MeV in the ^{238}U(γ, f) reaction and thereafter remains almost constant. The increase of the symmetric-product yield (Fig. 4) and the decrease of the P/V ratio (Fig. 5) clearly indicate the effect of the excitation energy. Further-
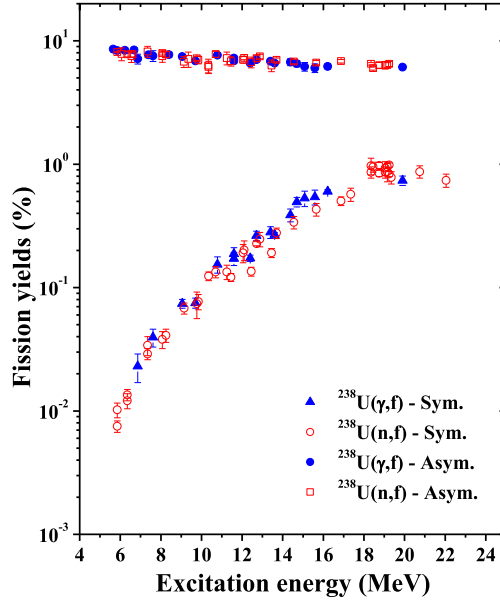
Fig. 4. Plot of yields of symmetric and asymmetric fission products (%) as a function of excitation energy in the ^{238}U(n, f) and ^{238}U(γ, f) reactions.
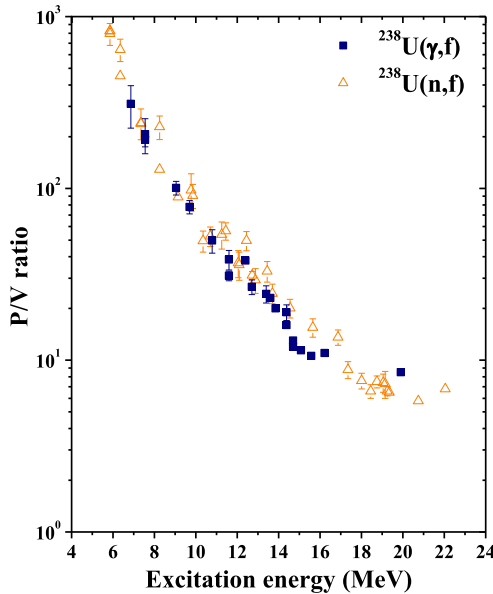

Fig. 5. Plot of peak-to-valley (P/V) ratio as a function of excitation energy in the ^{238}U(n, f) and ^{238}U(γ, f) reactions.

more, Fig. 4 shows that at the same excitation energy, the yields of the symmetric products are slightly higher in the ^{238}U(γ, f) reaction than in the ^{238}U(n, f) reaction. These causes a slightly lower P/V ratio in the ^{238}U(γ, f) reaction than in the ^{238}U(n, f) reaction (Fig. 5). Besides the

Table 6

Average light mass ($\langle A_L \rangle$), heavy mass ($\langle A_H \rangle$), and average neutron numbers ($\langle v \rangle_{\mathrm{expt}}$ in the neutron-induced fission of ^{238}U.

E_n (MeV)	E^* (MeV)	$\langle A_L \rangle$	$\langle A_H \rangle$	$\langle v \rangle_{\mathrm{expt}}$	Ref.
1.5	5.85	97.5	139	2.5	[25]
2.0	6.35	97.5	139	2.5	[25]
3.0	7.35	97.46	139	2.54	[20]
3.72	8.07	97.44	138.89	2.67	[35]
3.9	8.25	97.4	138.9	2.7	[25]
5.42	9.77	97.27	138.82	2.91	[35]
5.5	9.85	97.4	138.6	3.0	[25]
6.0	10.35	97.44	138.47	3.09	[24]
6.35	10.7	97.36	138.53	3.11	[A]
6.9	11.25	97.5	138.4	3.1	[25]
7.1	11.45	97.4	138.35	3.25	[24]
7.7	12.05	97.4	138.3	3.3	[25]
7.75	12.1	97.37	138.33	3.31	[35]
8.1	12.45	97.48	138.13	3.39	[24]
8.27	12.62	97.4	138.2	3.4	[27]
8.53	12.88	97.31	138.29	3.47	[A]
9.1	13.45	97.4	138.06	3.6	[24]
9.35	13.7	97.21	138.22	3.57	[A]
10.09	14.44	97.37	138.03	3.6	[35]
11.3	15.65	97.51	137.75	3.74	[30]
12.52	16.87	97.36	137.89	3.75	[A]
14.1	18.45	98.09	136.79	4.12	[19]
14.8	19.15	98.0	136.8	4.2	[21]

A – Present work.

role of the excitation energy, the difference may be due to the slightly lower outer fission barrier height of 5.7 MeV for the fissioning system of ^{238}U* compared to 6.12 MeV in ^{239}U* [84]. The lower height of the outer fission barrier for the fissioning system of ^{238}U* compared to ^{239}U* is due to the pairing effect. The role of the excitation energy above the outer fission barrier is clearly shown by Pomme et al. [58]. It was shown by them that the proton odd–even effect is nearly constant up to the excitation energy of 2.2 MeV above the outer fission barrier.

The role of excitation energy can also be seen in the average values of light mass ($\langle A_L \rangle$) and heavy mass ($\langle A_H \rangle$) as well as in the average neutron numbers in both the ^{238}U(n, f) and ^{238}U(γ, f) reactions. These values at average neutron energies of 6.35, 8.53, 9.35 and 12.52 MeV from the present work and at other lower-energies [8–35] are calculated from the mass-chain yields (Y_A) of the fission products within the mass ranges of 80–105 and 125–150, and by using the following relations,

$$\langle A_L \rangle = \sum (Y_A A_L) / \sum Y_A, \qquad \langle A_H \rangle = \sum (Y_A A_H) / \sum Y_A \qquad (8)$$

The obtained $\langle A_L \rangle$ and $\langle A_H \rangle$ values together with their corresponding average excitation energy ($\langle E^* \rangle$) in the ^{238}U(n, f) reaction are given in Table 6. From the $\langle A_L \rangle$, $\langle A_H \rangle$ and compound nucleus mass ($A_C = 239$), the experimental average numbers of neutrons ($\langle v \rangle_{\mathrm{expt}}$) were calculated according to the following relation:

$$\langle v \rangle_{\mathrm{expt}} = A_C - \left(\langle A_L \rangle + \langle A_H \rangle \right) \qquad (9)$$
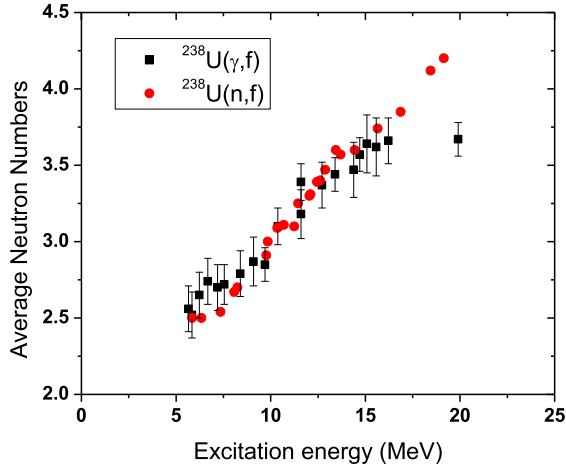
Fig. 6. Plot of average neutron numbers as a function of excitation energy in the ^{238}U(n, f) and ^{238}U(γ, f) reactions.

The obtained $\langle v \rangle_{\text{expt}}$ values from the present work and literature data in the ^{238}U(n, f) reaction [19–35] at different excitation energies are listed in Table 6. The $\langle v \rangle_{\text{expt}}$ values in the ^{238}U(n, f) reaction from Table 6 and literature data [42–63] in the ^{238}U(γ, f) reaction are plotted in Fig. 6 as a function of excitation energy. It can be seen from Fig. 6 that in the ^{238}U(n, f) and ^{238}U(γ, f) reactions, the value of $\langle v \rangle_{\text{expt}}$ increases with excitation energy. However, the increase trend of $\langle v \rangle_{\text{expt}}$ value with excitation energy is steeper in the ^{238}U(n, f) reaction than in the ^{238}U(γ, f) reaction. In the beginning up to excitation energy of 12.5 MeV, the value of $\langle v \rangle_{\text{expt}}$ is lower in the ^{238}U(n, f) reaction than in the ^{238}U(γ, f) reaction. This is most probably due to the slightly higher outer fission barrier height resulting from one extra odd-neutron in the fissioning system ^{239}U* than in the ^{238}U* as mentioned before. This means that the potential energy surface [85] is different between the compound nucleus ^{239}U* and ^{238}U* due to the single odd-nucleon in the former. Beyond the excitation energy of 12.5 MeV, the value of $\langle v \rangle_{\text{expt}}$ is slightly higher in the ^{238}U(n, f) reaction than in the ^{238}U(γ, f) reaction. This is because the average neutron number increases faster with excitation energy in the ^{238}U(n, f) reaction than in the ^{238}U(γ, f) reaction. This different behavior may be also due to the different types of interaction mechanism for neutron and photon besides the difference of outer fission barrier height between ^{239}U* and ^{238}U*. This can reflect in the yield profiles and thus in the $\langle A_L \rangle$ and $\langle A_H \rangle$ values. In order to examine this, the $\langle A_L \rangle$ and $\langle A_H \rangle$ values in the ^{238}U(n, f) reaction from Table 6 and literature data [42–63] in the ^{238}U(γ, f) reaction are plotted in Fig. 7 as a function of excitation energy.

It can be seen from Fig. 7 that in the ^{238}U(n, f) reaction, the $\langle A_H \rangle$ value almost remains constant around 139 up to the excitation energy of 10 MeV or decreases slightly from 139 at 6 MeV to 138.5 at 10 MeV. This is most probably due to the dominancy of the standard II over standard I asymmetric mode of fission or only first chance fission within the excitation energy of 10 MeV. The $\langle A_H \rangle$ value decreases significantly from the value of 138.5 at 10 MeV to 136.8 at 19 MeV due to the opening of the higher chance fission and dominancy of the standard I over the standard II asymmetric mode of fission. On the other hand, the $\langle A_L \rangle$ value remains nearly constant or increases slowly from 97.5 at 6 MeV to 98.09 at 18.45 MeV. In fact, the $\langle A_L \rangle$ value in the ^{238}U(n, f) reaction remains almost constant (97.5) from excitation energy of 5.85 MeV to 16.87 MeV and then slightly increases to the value of 98.09 at the excitation energy of 18.45 MeV. This is to conserve the mass of the fissioning system. As mentioned before, the
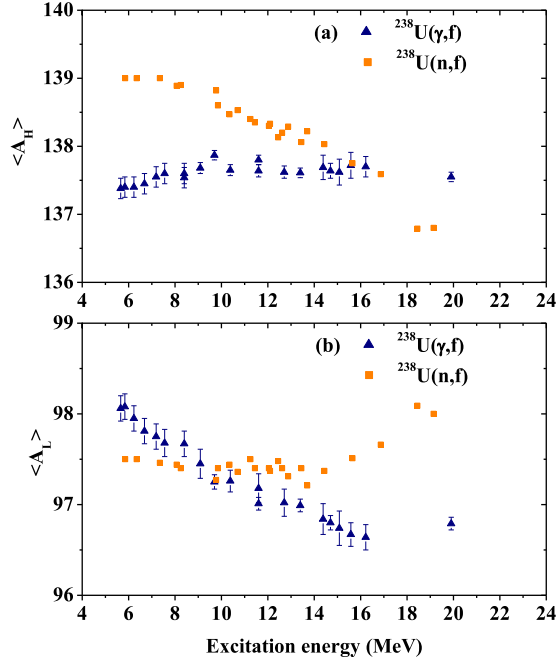
Fig. 7. Plot of average values of heavy mass ($\langle A_H \rangle$) and average values of light mass ($\langle A_L \rangle$) as a function of excitation energy in the ^{238}U(n, f) and ^{238}U(γ, f) reactions.

average neutron number ($\langle \upsilon \rangle_{\text{expt}}$) in the ^{238}U$(n, f)$ reaction also increases sharply with excitation energy. The sharp decrease of $\langle A_H \rangle$ and increase of $\langle \upsilon \rangle_{\text{expt}}$ indicates that in the ^{238}U(n, f) reaction, the increase of neutron emission with excitation energy is greater from the heavy fragments [25]. However, in the ^{238}U(γ, f) reaction, with increase of excitation energy, the $\langle A_L \rangle$ value decreases significantly from 98.1 to 96.8, whereas the $\langle A_H \rangle$ value remains nearly constant or increases slowly from 137.4 to 137.7. In fact in the ^{238}U(γ, f) reaction, the $\langle A_H \rangle$ value increases slightly within the excitation energy of 2.2 MeV above the outer barrier and then remains almost constant. However, it is surprising to see from Fig. 7, the reverse increasing or decreasing trend of the $\langle A_L \rangle$ and $\langle A_H \rangle$ values with excitation energy between the ^{238}U(n, f) and ^{238}U(γ, f) reactions. This is most probably due to the different types of interaction mechanism of neutron and photon with ^{238}U or due to the unpaired and paired neutron in between the fissioning systems ^{239}U* and ^{238}U*. Thus the partition of the excitation energy between collective and intrinsic degrees of freedom [69] is different for neutron and photon-induced fission of ^{238}U. This leads to the different role of the standard I and II asymmetric modes of the fission [68] based on the shell combination [69] of the complementary fragments between the ^{238}U(n, f) and ^{238}U(γ, f) reactions.

5. Conclusions

(i) The cumulative yields of various fission products in the 6.35, 8.53, 9.35 and 12.52 MeV quasi-mono-energetic-neutron induced fission of ^{238}U were determined by using an off-line γ-ray spectrometric technique. From the cumulative yields of fission products, their mass chain yields were obtained by using charge distribution corrections.

(ii) The yields of fission products for $A = 133$–134, $A = 138$–140, and $A = 143$–144 and their complementary products in the $^{238}U(n, f)$ and $^{238}U(\gamma, f)$ reactions are higher than those of other fission products. This is due to shell closure proximity based on standards I and II asymmetric mode of fission besides the role of even–odd effect.

(iii) In the $^{238}U(n, f)$ and $^{238}U(\gamma, f)$ reactions, the yields of high yield asymmetric products decrease marginally, whereas for the low-yield symmetric products increase significantly with excitation energies. Accordingly, the P/V ratio in both the cases decreases with excitation energy. This shows the role of excitation energy.

(iv) With the increase of excitation energy, the average neutron number ($\langle \upsilon \rangle$) increases significantly in the $^{238}U(n, f)$ reaction and slowly in the $^{238}U(\gamma, f)$ reaction. This different behavior is most probably due to slight higher outer fission barrier height resulting from one extra odd-neutron in the fissioning system $^{239}U^*$ compared to $^{238}U^*$.

(v) The $\langle A_H \rangle$ value in the $^{238}U(n, f)$ reaction and $\langle A_L \rangle$ value in the $^{238}U(\gamma, f)$ reaction decrease significantly with increase of excitation energy. On the other hand, $\langle A_L \rangle$ value in the $^{238}U(n, f)$ reaction and $\langle A_H \rangle$ value in the $^{238}U(\gamma, f)$ reaction increases slowly with increase of excitation energy to conserve the mass of the fissioning system. This different behavior may be due to the different types of interaction of neutron and photon with ^{238}U.

Acknowledgements

References

[1] K. Oyamatsu, H. Takeuchi, M. Sagisaka, J. Katakura, J. Nucl. Sci. Techol. 38 (2001) 477.
[2] T.R. Allen, D.C. Crawford, Lead-cooled fast reactor systems and the fuels and materials challenges, Sci. Technol. Nucl. Install. (2007), Article ID 97486, http://dx.doi.org/10.1155/2007/97486.
[3] Annual Project Status Report 2000, MIT-ANP-PR-071, INEFL/EXT-2009-00994.
[4] C. Wagemans, The Nuclear Fission Process, CRC, London, 1990.
[5] R. Vandenbosch, J.R. Huizenga, Nuclear Fission, Academic, New York, 1973.
[6] H. Naik, A.G.C. Nair, P.C. Kalsi, A.K. Pandey, R.J. Singh, A. Ramaswami, R.H. Iyer, Radiochim. Acta 75 (1996) 69.
[7] R.H. Iyer, H. Naik, A.K. Pandey, P.C. Kalsi, R.J. Singh, A. Ramaswami, A.G.C. Nair, Nucl. Sci. Eng. 135 (2000) 227.
[8] K.M. Brown, Phys. Rev. 126 (1962) 627.
[9] M.P. Menon, P.K. Kuroda, J. Inorg. Nucl. Chem. 26 (1964) 40.
[10] N.L. Borisova, S.M. Dubrovina, V.I. Novgorodtseva, V.A. Pchelin, V.A. Shigin, V.M. Shubko, Sov. J. Nucl. Phys. 6 (1968) 331.
[11] S.J. Lyle, J. Tillars, Radiochim. Acta 12 (1969) 43.
[12] D.J. Gorman, R.H. Tomilson, Can. J. Chem. 46 (1968) 1663.
[13] S.J. Lyle, J. Sellear, Radiochim. Acta 12 (1968) 43.
[14] S.J. Lyle, R. Wellum, Radiochim. Acta 13 (1969) 167.
[15] L.H. Gevaert, R.E. Jervis, H.D. Sharma, Can. J. Chem. 48 (1970) 641.
[16] S.G. Birgul, S.J. Lyle, R. Wellum, Radiochim. Acta 16 (1971) 104.
[17] J.P. Bocquet, Nucl. Phys. 189 (1972) 556.
[18] D.R. Nethaway, B. Mendoza, Phys. Rev. C 6 (1972) 1821, 1827.
[19] J. Blachot, L.C. Carraz, P. Cavalini, C. Chauvin, A. Ferrieu, A. Moussa, J. Inorg. Nucl. Chem. 36 (1974) 495.
[20] J.T. Harvey, D.E. Adams, W.D. James, J.N. Beck, J.L. Meason, P.K. Kuroda, J. Inorg. Nucl. Chem. 37 (1975) 2243.

[21] D.E. Adams, W.D. James, J.N. Beck, P.K. Kuroda, J. Inorg. Nucl. Chem. 37 (1975) 419.
[22] M. Rajagopalan, H.S. Pruys, A. Grutter, E.A. Hermes, H.R. von Gunten, J. Inorg. Nucl. Chem. 38 (1976) 351.
[23] S. Daroczy, P. Raics, S. Nagy, L. Koever, I. Hamvas, E. Gorman, Atomki Cozcmenyek 18 (1976) 317.
[24] T.C. Chapman, G.A. Anzelon, G.C. Spitale, D.R. Nethaway, Phys. Rev. C 17 (1978) 1089.
[25] S. Nagy, K.F. Flynn, J.E. Gindler, J.W. Meadows, L.E. Glendenin, Phys. Rev. C 17 (1978) 163.
[26] L. Wexin, S. Tongyu, Z. Manjiao, D. Tianrong, S. Xiuhua, He Huaxue, Yu F. Huakue, High Energy Phys. Nucl. Phys. 2 (1980) 9, High Energy Phys. Nucl. Phys. 5 (1983) 176 (in Chineese).
[27] L. Ze, Z. Chunhua, L. Conggui, W. Xiuzhi, Q. Limkun, C. Anzhi, L. Huijung, Z. Sujing, L. Yonghui, Ju Changxin, L. Daming, T. Peija, M. Jiangchen, J. Kixing, High Energy Phys. J. Nucl. Phys. 7 (1985) 97 (in Chineese).
[28] L. Conggui, L. Huijun, L. Yonghui, High Energy Phys. Nucl. Phys. 7 (1985) 235 (in Chineese).
[29] A. Afarideh, K.R. Annole, Ann. Nucl. Energy 16 (1989) 313.
[30] Z. Li, X. Wang, K. Jing, A. Cui, D. Liu, S. Su, P. Tang, T. Chih, S. Zhang, J. Gao, Radiochim. Acta 64 (1994) 95.
[31] G. Lhersonnau, P. Denloov, G. Canchel, J. Huikari, J. Jardin, A. Tokinen, V.K. Olhinen, C. Lau, L. Lebroton, A.C. Mueller, A. Nieminen, S. Nummela, H. Penttila, K. Perajavi, Z. Radivojevic, V. Rubchenya, M.G. Saint-Laurent, W.H. Trzaska, D. Vakhtin, J. Vervier, A.C. Villari, J.C. Viang, J. Aystoe, Eur. Phys. J. A 9 (2000) 385.
[32] I. Clenk, Radiochim. Acta 85 (1999) 85;
    I. Clenk, Radiochim. Acta 89 (2001) 481.
[33] J. Laurec, A. Adam, T. DeBruyne, E. Brauge, T. Granier, J. Aupiais, O. Barsillon, G. Lepetit, N. Authier, P. Casoli, Nucl. Data Sheets 111 (2010) 2965.
[34] I.V. Ryzhov, S.G. Yavshits, G.A. Tutin, N.V. Kovalev, A.V. Saulski, N.A. Kudryashev, M.S. Onegin, L.A. Vaishnene, Yu.A. Gavrikov, O.T. Grudzevich, V.D. Simutkin, S. Pomp, J. Blomgren, M. Osterlund, P. Andersson, R. Bevilacqua, J. Meulders, R. Prieels, Phys. Rev. C 83 (2011) 054603.
[35] H. Naik, V.K. Mulik, P.M. Prajapati, B.S. Shivasankar, S.V. Suryanarayana, K.C. Jagadeesan, S.V. Thakare, S.C. Sharma, A. Goswami, Nucl. Phys. A 913 (2013) 185.
[36] E.A.C. Crouch, At. Data Nucl. Data Tables 19 (1977) 417.
[37] A.C. Wahl, At. Data Nucl. Data Tables 39 (1988) 1.
[38] B.F. Rider, Compilation of fission products yields, NEDO, 12154 3c ENDF-327, Valecicecitos Nuclear Centre, 1981.
[39] J.R. England, B.F. Rider, Evaluation and compilation of fission products yields, in: ENDF/BVI, 1989, 1992.
[40] M. James, R. Mills, Neutron fission products yields, UKFY2 1991, JEF-2.2 1993.
[41] IAEA-EXFOR Database, at http://www-nds.iaea.org/exfor.
[42] R.A. Schmitt, N. Sugarman, Phys. Rev. 95 (1954) 1260.
[43] H.G. Richter, C.D. Coryell, Phys. Rev. 95 (1954) 1550.
[44] L. Katz, T.M. Kavanagh, A.G.W. Cameron, E.C. Bailey, J.W.T. Spinks, Phys. Rev. 99 (1958) 98.
[45] J.L. Meason, P.K. Kuroda, Phys. Rev. 142 (1966) 691.
[46] I.R. Willams, C.B. Fulmer, G.F. Dell, M.J. Engebretson, Phys. Lett. B 26 (1968) 140.
[47] L.H. Gevaert, R.E. Jervis, S.C. Subbarao, H.D. Sharma, Can. J. Chem. 48 (1970) 652.
[48] B. Schrøder, G. Nydahl, B. Forkman, Nucl. Phys. A 143 (1970) 449.
[49] A. Chattopadhyay, K.A. Dost, I. Krajbich, H.D. Sharma, J. Inorg. Nucl. Chem. 35 (1973) 2621.
[50] D. Swindle, R. Wright, K. Takahashi, W.H. Rivera, L. Meason, Nucl. Sci. Eng. 52 (1973) 466.
[51] A. De Clercq, E. Jacobs, D. De Frenne, H. Thierens, P. D'hondt, A.J. Deruytter, Phys. Rev. C 13 (1976) 1536.
[52] H. Thierens, D. De Frenne, E. Jacobs, A. De Clercq, P. D'Hondt, A.J. Deruytter, Phys. Rev. C 14 (1976) 1058.
[53] W.D. James, D.E. Adams, R.A. Sigg, J.T. Harvey, J.L. Meason, J.N. Beck, P.K. Kuroda, H.L. Wright, J.C. Hogan, J. Inorg. Nucl. Chem. 38 (1978) 1109.
[54] E. Jacobs, H. Thierens, A. De Frenne, A. De Clercq, P. D'Hondt, P. De Gelder, A.J. Deruytter, Phys. Rev. C 19 (1979) 422.
[55] E. Jacobs, A. De Clercq, H. Thierens, D. De Frenne, P. D'hondt, P. De Gelder, A.J. Deruytter, Phys. Rev. C 20 (1979) 2249.
[56] E. Jacobs, H. Thierens, D. De Frenne, A. De Clercq, P. D'Hondt, P. De Gelder, A.J. Deruytter, Phys. Rev. C 21 (1980) 237.
[57] A. Yamadera, T. Kase, T. Nakamura, in: Proceedings of the International Conference on Nuclear Data for Science and Technology, Moto, Japan, 1988, Japan Atomic Energy Research Institute, Tokai, Japan, 1988, p. 1147.
[58] S. Pomme, E. Jacobs, K. Persyn, D. De Frenne, K. Govaert, M.L. Yoneama, Nucl. Phys. A 560 (1993) 689.
[59] S. Pomme, E. Jacobs, M. Piessens, D. De Frenne, K. Persyn, K. Govaert, N.-L. Yoneama, Nucl. Phys. A 572 (1994) 237.
[60] K. Persyn, E. Jacobs, S. Pomme, D. De Frenne, K. Govaert, M.-L. Yoneama, Nucl. Phys. A 615 (1997) 198.

[61] A. Gook, M. Chernykh, C. Eckardt, J. Enders, P. von Neumann-Cosel, A. Oberstedt, S. Oberstedt, A. Richter, Nucl. Phys. A 851 (2011) 1.
[62] H. Naik, V.T. Nimje, D. Raj, S.V. Suryanarayana, A. Goswami, S. Singh, S.N. Acharya, K.C. Mittal, S. Ganesan, P. Chandrachoodan, V.K. Manchanda, V. Venugopal, S. Banarjee, Nucl. Phys. A 853 (2011) 1.
[63] H. Naik, Frédérick Carrel, G.N. Kim, Frédéric Laine, Adrien Sari, S. Normand, A. Goswami, Eur. Phys. J. A 49 (2013) 94.
[64] K.-H. Schmidt, S. Steinhauser, C. Bockstiegel, A. Rewe, A. Heinz, A.R. Junghans, J. Benlliure, H.-G. Clerc, M. de Jong, J. Muller, M. Pfutzner, B. Voss, Nucl. Phys. A 665 (2000) 211.
[65] S. Steinhauser, J. Benlliure, C. Bockstiegel, H.-G. Clerc, A. Heinz, A. Rewe, M. de Jong, A.R. Junghans, J. Muller, M. Pfutzner, K.-H. Schmidt, Nucl. Phys. A 634 (1998) 89.
[66] J. Benlliure, A.R. Junghans, K.-H. Schmidt, Eur. Phys. J. A 13 (2002) 93.
[67] H. Naik, R.J. Singh, R.H. Iyer, Eur. Phys. J. A 16 (2003) 495.
[68] U. Brosa, S. Grossmann, A. Muller, Phys. Rep. 197 (1990) 167.
[69] B.D. Wilkins, E.P. Steinberg, R.R. Chasman, Phys. Rev. C 14 (1976) 1832.
[70] H. Umezawa, S. Baba, H. Baba, Nucl. Phys. A 160 (1971) 65.
[71] H. Naik, S.V. Suryanarayana, V.K. Mulik, P.M. Prajapati, B.S. Shivashankar, K.C. Jagadeesan, S.V. Thakare, D. Raj, S.C. Sharma, P.V. Bhagwat, S.D. Dhole, V.N. Bhoraskar, A. Goswami, J. Radioanal. Nucl. Chem. 293 (2012) 469.
[72] Sadhana Mukerji, H. Naik, S.V. Surayanarayana, B.S. Shivashankar, V.K. Mulik, Sachin Chachara, Sudipta Samanta, A. Goswami, P.D. Krishnani, J. Basic Appl. Phys. 2 (2013) 104.
[73] R. Crasta, S. Ganesh, H. Naik, A. Goswami, S.V. Suryanarayana, S.C. Sharma, P.V. Bhagwat, B.S. Shivashankar, V.K. Mulik, P.M. Prajapati, Nucl. Sci. Eng. 178 (2014) 1.
[74] J.F. Ziegler, J.P. Biersack, U. Littmark, SRIM 2003 Code. The Stopping and Range of Ions in Solids, Pergamon, New York, 2003.
[75] C.H. Poppe, J.D. Anderson, J.C. Davis, S.M. Grimes, C. Wong, Phys. Rev. C 14 (1976) 438.
[76] H. Liskien, A. Paulsen, At. Data Nucl. Data Tables 15 (1975) 57.
[77] J.W. Meadows, D.L. Smith, Neutrons from proton bombardment of natural Lithium, Argonne National Laboratory Report ANL-7983, 1972.
[78] J.K. Tuli, Nuclear Wallet Cards, National Nuclear Data Center, Brookhaven National Laboratory, Upton, New York 11973-5000, USA (2006).
[79] E. Browne, R.B. Firestone, in: V.S. Shirley (Ed.), Table of Radioactive Isotopes, Wiley, New York, 1986; R.B. Firestone, L.P. Ekstrom, in: Table of Radioactive Isotopes, 2004, Version 2.1, http://ie.lbl.gov/toi/index.asp.
[80] J. Blachot, C. Fiche, Ann. Phys. Suppl. 6 (1981) 3.
[81] N. Sugarman, A. Turkevich, in: C.D. Coryell, N. Sugarman (Eds.), Radiochemical Studies: The Fission Product, vol. 3, McGraw–Hill, New York, 1951, p. 1396.
[82] M. Haddad, J. Crancon, G. Lhospice, M. Asghar, J. Blachot, Radiochim. Acta 42 (1987) 165.
[83] C. Agarwal, A. Goswami, P.C. Kalsi, S. Singh, A. Mhatre, A. Ramaswami, J. Radioanal. Nucl. Chem. 275 (2008) 445.
[84] S. Bjornholm, J.E. Lynn, Rev. Mod. Phys. 52 (1980) 725.
[85] P. Moller, Nucl. Phys. A 192 (1972) 529.